Supplement of The Cryosphere, 10, 15–27, 2016
http://www.the-cryosphere.net/10/15/2016/
doi:10.5194/tc-10-15-2016-supplement

The Cryosphere Open Access EGU

Supplement of

Estimating supraglacial lake depth in West Greenland using Landsat 8 and comparison with other multispectral methods

A. Pope et al.

Correspondence to: A. Pope (allen.pope@post.harvard.edu)

We calculate g (the coefficient related to losses in upward and downward travel through the water column, units: m^{-1}) beginning with a relationship from Smith and Baker (1981, Eq. 5):

$$K = a + \tfrac{1}{2}b \quad \text{(S1)}$$

where K is the diffuse attenuation coefficient for water, a is the absorption coefficient for water, and b is the backscattering coefficient for molecular (Rayleigh) scatter in water. Treating this as an equality yield "the lowest experimental value one could expect to encounter in natural freshwater based on laboratory measured values of the inherent optical properties for pure water." Then, we plug this into Sneed and Hamilton (2007, Eq. 3):

$$g \approx K + aD_u \quad \text{(S2)}$$

where D_u is an upwelling light distribution function or the reciprocal of the upwelling average cosine. By applying the assumption from Maritorena et al. (1994) that $K_d \approx aD_u$, we arrive at the following relationship between measured values (a and b) and g:

$$g = 2a + b \quad \text{(S3)}$$

To calculate g, we use an updated absorption coefficient (a) from Pope and Fry (1997, Table 3) to replace the previously used a from Smith and Baker (1981, Table 1). We also use scattering coefficient (b) from Buiteveld et al. (1994, Table 1) and OLI's relative spectral response function (Barsi et al., 2014) to created an appropriately weighted average g for each OLI band. See Tables 1 and S1 for calculated values of g.

Table S1. Laboratory-based and in situ-derived water absorption coefficients for lake depth estimation using the physically based method (*g*, see Eqn. 1) and empirical method (*a*, *b*, and *c*, see Eqns. 5-6). Regression statistics for lake depth estimates using field spectra convolved to emulate multispectral bands (correlation coefficient and root mean squared error) are also included.

Satellite & Band	Lab-based *g* (m^{-1})	Regressed *g* (m^{-1})	*r*	RMSE (m)
ASTER 1 (green) Gain H	0.1584	0.15	0.7687	0.83
ASTER 1 (green) Normal	0.1584	0.15	0.7688	0.83
ASTER 1 (green) Gain L	0.1584	0.15	0.7675	0.83
ASTER 2 (red) Gain H	0.8183	0.82	0.9551	0.31
ASTER 2 (red) Normal	0.8183	0.80	0.9375	0.38
ASTER 2 (red) Gain L	0.8183	0.80	0.9532	0.32
MODIS 1 (red)	0.6922	1.00	0.9346	1.62
MODIS 3 (blue)	0.0235	0.02	0.1424	5.27
MODIS 4 (green)	0.1181	0.25	0.7375	0.93
WV2 1 (coastal)	0.0159	0.01	0.0244	12.60
WV2 2 (blue)	0.0317	0.03	0.2487	3.49
WV2 3 (green)	0.1144	0.13	0.7271	0.95
WV2 4 (yellow)	0.4749	0.51	0.9400	0.36
WV2 5 (red)	0.7865	0.81	0.9627	0.28
WV2 6 (red-edge)	2.1542	1.00	0.9134	0.41

Table S2. List of satellite imagery used in this paper's analysis.

Landsat 8 Imagery

Path	Row	DOY	Year
023	006	183	2013
023	006	199	2013
023	006	215	2013
023	006	231	2013
006	012	163	2014
006	012	195	2014
006	012	211	2014
006	013	163	2014
006	013	195	2014
006	013	211	2014
006	013	245	2014
006	014	163	2014
006	014	195	2014
006	014	211	2014
006	014	542	2014
006	015	163	2014
006	015	195	2014
006	015	211	2014
006	015	243	2014
007	012	218	2014
007	013	218	2014
007	014	170	2014
007	014	218	2014
008	011	161	2014
008	011	193	2014
008	012	161	2014
008	012	193	2014
009	011	152	2014
009	011	184	2014

009	011	200	2014
009	011	216	2014
009	012	152	2014
009	012	184	2014
009	012	216	2014
010	012	159	2014
010	012	207	2014
010	012	223	2014
010	012	239	2014

WorldView Stereo Imagery

Northwest or Sermeq Kujalleq (Jakobshavn)	Sensor	Date *YYYY/MM/DD*	Scene 1	Scene 2
SK / Jakobshavn	WV-1	2013/07/05	102001002326E500	1020010024E0E700
SK / Jakobshavn	WV-2	2013/07/22	1030010024C6FC00	10300100245A7F00
SK / Jakobshavn	WV-2	2013/07/22	1030010025666700	1030010025C69600
SK / Jakobshavn	WV-2	2013/08/04	103001002757A900	10300100258CFE00
SK / Jakobshavn	WV-2	2013/08/19	1030010025CF8000	103001002591E600
SK / Jakobshavn	WV-2	2013/09/29	1030010027356800	1030010027356800
Northwest	WV-1	2012/03/12	1020010018240600	10200100195C7600
Northwest	WV-1	2013/03/22	1020010021B0C500	1020010021E40100
Northwest	WV-1	2013/03/26	102001002289F900	1020010020A0AB00
Northwest	WV-1	2013/07/19	10200100224D0500	1020010021E40100
Northwest	WV-1	2013/08/10	1020010024637300	1020010025955F00
Northwest	WV-2	2013/09/29	1030010027967F00	10300100276B3E00

As an experiment, WorldView Stereo DEMs were also used to calibrate all necessary coefficients for both the physically based and empirical methods (as opposed to using any information from the scene itself, such as ice albedo and optically deep water). Both ETM+ and OLI produced successful results with low errors with a variety of bands and band combinations (see Fig. S1 & Table S2). Only TOA reflectance was used in these regressions. Despite being collected on different days over separate sites, the ETM+ and OLI coefficients are very similar (see Fig. S2, Table S3). However, because all parameters are free, they are not directly comparable to the coefficients used in the rest of this study. Still, a wider range of lakes is likely necessary to build robust coefficients for ice sheet-wide application.

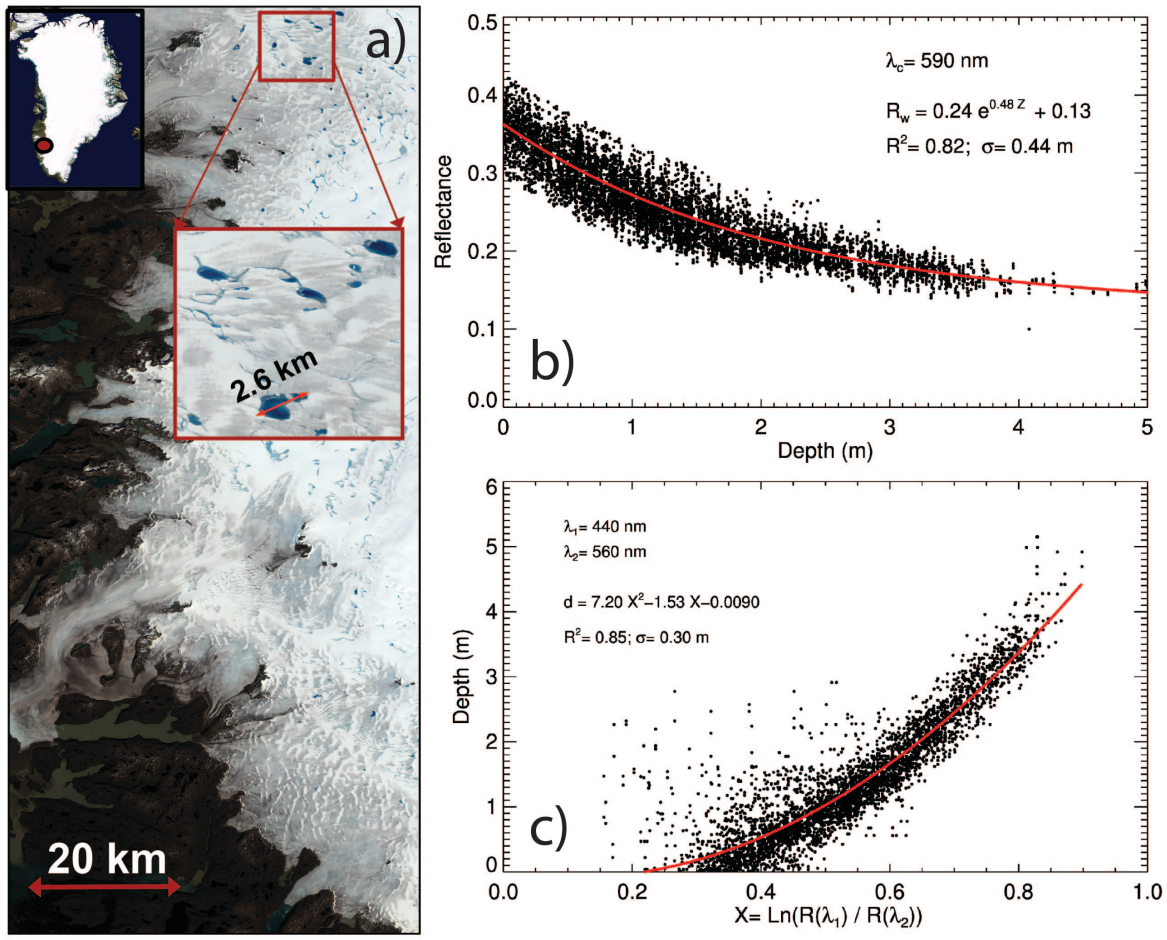

Figure S1. a) Map showing Landsat 8 OLI image and lakes used for calibration and validation. b) Water-leaving reflectance measured from OLI Band 8 (panchromatic) vs. post-drainage depths. c) Image-derived radiometric quantity measured from L8 OLI's coastal blue (Band 1) and green (Band 3) channels vs. post-drainage depths.

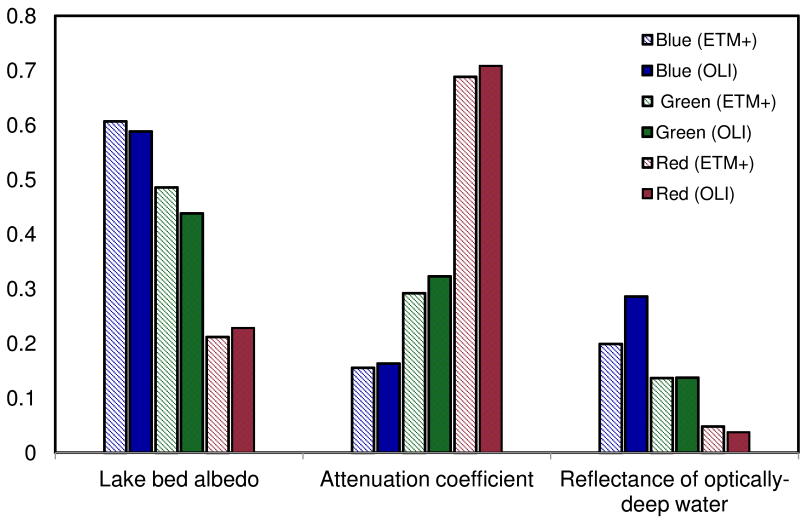

Figure S2. Physically based single-band coefficients for OLI and ETM+ sensors based on imagery collected over two separate sites and different days.

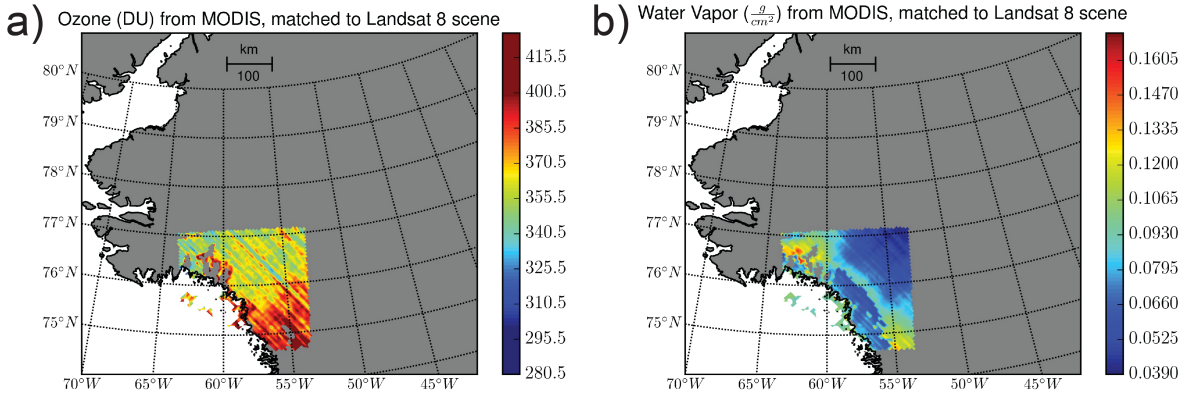

Figure S3 MODIS (a) ozone and (b) water vapor retrievals used for MODTRAN radiative transfer model sensitivity assessment of lake depth retrievals to path radiance on 18 July 2013. Data extent clipped to Landsat area of interest for northwest Greenland study region.

Table S3. Statistics on depth-retrieval based on OLI image data using various single- and dual-band methods.

Band(s)	Mean Error (m)	RMSE (m)	r^2	Volumetric Error (%)
1 - Coastal	-0.39	1.19	0.52	27.3
2 – Blue	-0.24	0.91	0.72	16.3
3 – Green	-0.08	0.47	0.94	5.9
4 – Red	-0.22	0.43	0.93	14.0
8 - Pan	-0.10	0.45	0.96	7.2
1 / 3	0.01	0.29	0.99	0.60
1 / 4	0.00	0.45	0.99	1.98
1 / 8	0.00	0.39	0.99	1.03
2 / 3	0.01	0.30	0.99	0.66
2 / 8	0.00	0.42	0.99	2.07

Table S4. Landsat 7 and Landsat 8 coefficients for the physically based single-band model, as derived from the small training set described above. All parameters were left free.

Band	Parameter	Landsat 7 (ETM+)	Landsat 8 (OLI)
Blue	A_d	0.6071	0.5882
	g	0.1556	0.1632
	R_∞	0.1992	0.2861
Green	A_d	0.48589045	0.4384
	g	0.29202123	0.3231
	R_∞	0.13680709	0.1375
Red	A_d	0.21199443	0.2284
	g	0.68851528	0.7083
	R_∞	0.047975375	0.0375

References

Barsi, J. A., Lee, K., Kvaran, G., Markham, B. L. and Pedelty, J. A.: The Spectral Response of the Landsat-8 Operational Land Imager, Remote Sens., 6(10), 10232–10251, doi:10.3390/rs61010232, 2014.

Buiteveld, H., Hakvoort, J. H. M. and Donze, M.: Optical properties of pure water, vol. 2258, pp. 174–183., 1994.

Maritorena, S., Morel, A. and Gentili, B.: Diffise reflectance of oceanic shallow waters: Influence of water depth and bottom albedo, Limnol. Oceanogr., 39(7), 1689–1703, 1994.

Pope, R. M. and Fry, E. S.: Absorption spectrum ~380–700 nm! of pure water. II. Integrating cavity measurements, Appl. Opt., 36(33), 8710–8723, 1997.

Smith, R. C. and Baker, K. S.: Optical properties of the clearest natural waters (200-800 nm), Appl. Opt., 20(2), 177–184, 1981.

Sneed, W. A. and Hamilton, G.: Evolution of melt pond volume on the surface of the Greenland Ice Sheet, Geophys. Res. Lett., 34, L03501, 2007.